Spectrochimica Acta Part A: Molecular and Biomolecular Spectroscopy 132 (2014) 713–725

Contents lists available at ScienceDirect

Spectrochimica Acta Part A: Molecular and Biomolecular Spectroscopy

journal homepage: www.elsevier.com/locate/saa

Theoretical (in B3LYP/6-3111++G** level), spectroscopic (FT-IR, FT-Raman) and thermogravimetric studies of gentisic acid and sodium, copper(II) and cadmium(II) gentisates

E. Regulska [a,*], M. Kalinowska [a], S. Wojtulewski [b], A. Korczak [c], J. Sienkiewicz-Gromiuk [d], Z. Rzączyńska [d], R. Świsłocka [a], W. Lewandowski [a]

[a] Division of Chemistry, Bialystok University of Technology, Zamenhofa 29, 15-435 Bialystok, Poland
[b] Institute of Chemistry, University of Bialystok, Hurtowa 1, 15-399 Bialystok, Poland
[c] Institut des Sciences et Techniques, Université de Valenciennes et du Hainaut-Cambrésis, France
[d] Department of General and Coordination Chemistry, Faculty of Chemistry UMCS, Sq. Maria Curie-Skłodowska 2, Lublin, Poland

HIGHLIGHTS

- The formulas of synthesized complexes were determined.
- The monodentate type of coordination in Cu/Cd gentisates was established.
- The molecular structures were discussed.
- FT-IR and Raman spectra were studied.

ARTICLE INFO

Article history:
Received 24 January 2014
Received in revised form 23 April 2014
Accepted 30 April 2014
Available online 16 May 2014

Keywords:
2,5-Dihydroxybenzoic acid
Gentisic acid
Metal 2,5-dihydroxybenzoate
DFT calculations
FT-IR
FT-Raman

GRAPHICAL ABSTRACT

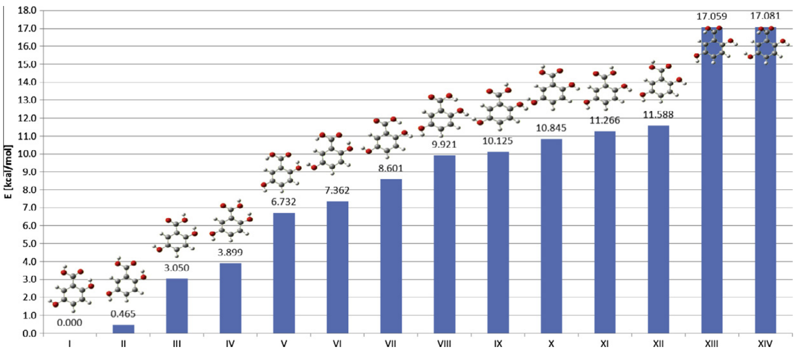

ABSTRACT

The DFT calculations (B3LYP method with 6-311++G(d,p) mixed with LanL2DZ for transition metals basis sets) for different conformers of 2,5-dihydroxybenzoic acid (gentisic acid), sodium 2,5-dihydroxybenzoate (gentisate) and copper(II) and cadmium(II) gentisates were done. The proposed hydrated structures of transition metal complexes were based on the results of experimental findings. The theoretical geometrical parameters and atomic charge distribution were discussed. Moreover Na, Cu(II) and Cd(II) gentisates were synthesized and the composition of obtained compounds was revealed by means of elemental and thermogravimetric analyses. The FT-IR and FT-Raman spectra of gentisic acid and gentisates were registered and the effect of metals on the electronic charge distribution of ligand was discussed.

Introduction

Gentisic acid (2,5-dihydroxybenzoic acid = 2,5-DHBA) belongs to the group of phenolic acids, substances that naturally occur in fruit, vegetables, nuts, seeds, flowers and some herb beverages. It

---

* Corresponding author. Tel.: +48 797 995 975.
E-mail address: e.regulska@pb.edu.pl (E. Regulska).

http://dx.doi.org/10.1016/j.saa.2014.04.191
1386-1425/

was found in citrus fruits (*Citrus* spp.), grapes (*Vitis vinifera*), Jerusalem artichoke (*Helianthus tuberosus*), sesame (*Sesamum indicum*), gentians (*Gentiana* spp.), red sandalwood (*Pterocarpus santalinus*), rose gum (*Eucalyptus grandis*), saxifrage (*Saxifraga* spp.) and olive (*Olea europaea*) [1]. 2,5-DHBA is an active metabolite of salicylic acid degradation. It shows a broad spectrum of biological activity such as anti-inflammatory, anti-rheumatic, antioxidant and antibacterial properties [2,3]. Cunha et al. [4] examined pharmacological mechanism of relaxation caused by gentisic acid in the guinea pig trachea. It is believed that gentisic acid has an effective role in the anticarcinogenetic activity of *China-rose hibiscus* (*Hibiscus rosa-sinensis*) extract [5]. Ashidate et al. [6] report that gentisic acid inhibits low-density lipoprotein oxidation and the formation of cholesterol ester hydroperoxides in human plasma. They also suggest that its antioxidant properties are mainly due to its radical scavenging activity. A recent study has shown that gentisic acid is a Fibroblast Growth Factor (FGF) inhibitor [7]. Dihydroxybenzoic acids are plant secondary metabolites naturally present in almost all plant materials, including food products of plant origin and other substances such as propolis [8]. In industrial field they are used as intermediates for production of pharmaceuticals and other organic chemicals: resins, polyesters, plasticizers, dyestuffs, preservatives and rubber chemicals. According to Vraslović et al. [2] gentisic acid acts as a cathodic inhibitor of the Al-2,5Mg alloy. The inhibitory action of gentisic acid was explained by the formation of complex molecules with aluminum ions and then precipitation of these complexes on alloy surface in places where oxide film was destroyed. Sodium gentisate (Na 2,5-DHB) is known for its pharmacological properties like anti-inflammatory, analgesic and antipyretic drugs [9]. Gentisic acid forms also complexes with transition metals. Interaction of such metal ions as Mn(II), Co(II), Ni(II), Cu(II) and Cd(II) with 2,5dihydroxybenzoic acid was presented by Micera et al. [10]. Crystals suitable for X-ray analysis they obtained only in the case of Zn complex. It's crystalline structure (Fig. 1) was presented as [Zn(2,5-DHB)$_2$(H$_2$O)$_4$] compound [10]. Other metals formed similar complexes with exception of copper, which was described as [Cu(2,5-DHB)$_2$(H$_2$O)$_2$]·2H$_2$O. Although Sokolik et al. [11] defined copper gentisate as [Cu(2,5-DHB)$_2$(H$_2$O)$_4$] complex. They described the syntheses of copper(II) 2,4-, 2,5- and 2,6-dihydroxybenzoates. Presented analytical data of thermogravimetric analyses, magnetic moments as well as the electronic and EPR spectra showed that 2,4- and 2,6-dihydroxybenzoic acids formed octahydrated complexes with copper(II) unlike gentisic acid. Furthermore all compounds exhibited higher anti-inflammatory activities on dextran edema than free carboxylic acids. Ashidate et al. [6] basing on UV spectra mentioned without publishing any data that gentisic acid had only minimal copper chelating activity. According to Micera et al. [12] copper(II) always displays a different coordination behavior in comparison with Mn, Co, Ni and Zn divalent ions, which all exhibit very similar coordination geometries. The authors studied interaction of metal ions with 2,4-, 2,5- and 2,6-dihydoxybenzoic acids and concluded that phenolic groups show a tendency to be involved in hydrogen-bonding rather than in metal coordination. On the other hand the ligands have different tendencies when they taking part in the inner coordination sphere of metal ions. Metal–ligand interactions of outer-sphere nature are allowed with 2,6-DHBA, whereas for 2,4- and 2,5-DHBs coordinative properties are more typical for carboxylate ligands. Synthesis and characterization of Mo(VI) complexes of 2,3- and 2,5-DHBA as polyoxometallate species having Mo$_2$O$_5$/MoO$_2$ core were described by Karaliota et al. [13]. According to Litos et al. [14] gentisic acid acts as tridentate ligand using both carboxyl oxygen atoms, giving trinuclear oxomolybdenum complex. Each ligand coordinates with three molybdenum atoms. The hydroxyl-oxygen of the carboxylate group acts as a bridge between two molybdenum atoms, while the third molybdenum atom coordinates with the carbonyl-oxygen. The two hydroxyl non-bonded groups of the ligands participate in hydrogen bonding interactions. This structure was characterized as unusual in contrast to salicylate (bidentate) coordination type.

In the present study the synthesis of sodium, copper(II) and cadmium(II) gentisates, the evaluation of the their composition

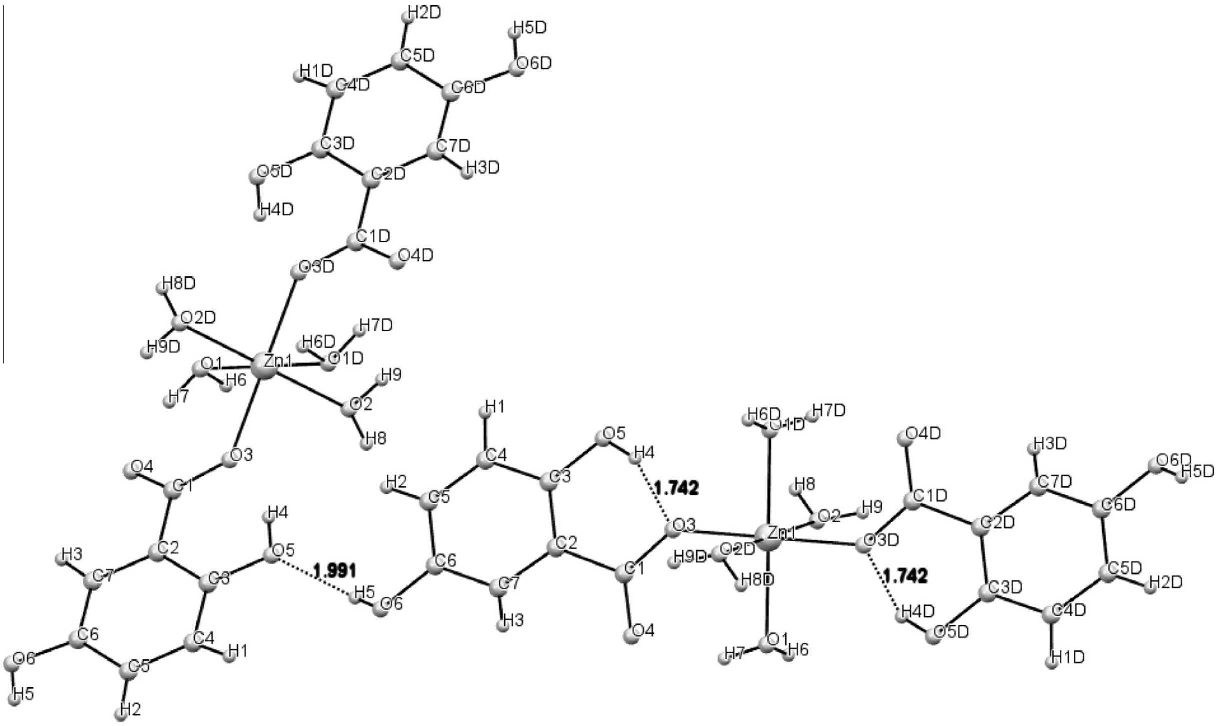

Fig. 1. Crystalline structure of zinc gentisate (the hydrogen bonds are highlighted the dotted lines) [10].

and the investigation using vibrational spectroscopy, as well as quantum-chemical calculations are described.

Experimental

Sodium 2,5-dihydroxybenzoate was prepared by dissolving the powder of gentisic acid in the water solution of sodium hydroxide in a stoichiometric ratio (1:1). Water solution of copper or cadmium chlorides was added to aqueous solution of sodium gentisate in a stoichiometric ratio (1:2). The obtained precipitates were filtered off and washed with distilled water and then dried several hours at about 65 °C. The precipitate of cadmium gentisate was water-soluble but copper gentisate was insoluble in water.

Elemental analysis for the weight percentages of carbon and hydrogen was done with Perkin–Elmer 240 equipment. The thermal stability and decomposition of copper and cadmium gentisates were examined using a Setsys 16/18 (Setaram) thermal analyzer recording the TG/DSC/DTG curves. The samples (8–9 mg) were heated in a ceramic crucible between 30–1000 °C [Cd(II) complex] or 30–750 °C [Cu(II) compound] in flowing air atmosphere with a heating rate of 5 °C/min. The products of dehydration and decomposition processes were established on the basis of the TG curves. FT-IR spectra were recorded with the Equinox 55 Bruker FT-IR spectrometer within the range 4000–400 cm^{-1}. Samples in the solid state were measured in KBr matrix. Pellets were obtained with a hydraulic press under 739 MPa pressure. FT-Raman spectra of solid samples in capillary tubes were recorded in the range of 4000–400 cm^{-1} with a FT-Raman accessory of Bruker MultiRAM. The resolution of spectrometer was 1 cm^{-1}.

The calculations were carried out with the Gaussian09 set of codes [15]. The B3LYP functional with Pople type basis set (6-311++G(d,p)) was applied. The gentisic acid, sodium salt and its tautomeric forms were optimized and no imaginary frequencies were found. In case of copper and cadmium complexes the optimization were carried out with use of the same DFT method coupled with mixed basis set: 6-311++G(d,p) for C, O, and H atoms, and LanL2DZ for transition metals.

Results and discussion

Synthesized complexes composition

The results of elemental and thermogravimetric analyses are gathered in Table 1. Thermogravimetric analysis was performed to investigate the thermal stability and to describe the way of decomposition of copper and cadmium complexes. The results obtained from their thermal decomposition show that studied gentisates are hydrated salts. The data of thermal decomposition are listed in Table 2. Thermoanalytical curves of copper and cadmium complexes (Fig. 2) are presented to indicate that in the case of each individual complex occurs the various numbers of stages of dehydration process and degradation of organic ligand. The thermal analysis data show that the number of water molecules is in good agreement with that defined by elemental analysis ($[Cu(C_7H_5O_4)_2]\cdot4H_2O$ and $[Cd(C_7H_5O_4)_2]\cdot4H_2O$). Moreover the metal percentages calculated from the metal oxide residues were also found to be in good agreement with the results of elemental analysis (Table 1). The $[Cu(C_7H_5O_4)_2]\cdot4H_2O$ complex heated in the temperature range of 30–150 °C dehydrates and forms an anhydrous complex (Fig. 2a). The relative mass loss calculated from TG curve being equal to 16.22% corresponds to the loss of four molecules of water (calculated value is 16.31%). In the temperature range of 150–410 °C the anhydrous gentisate of Cu(II) is finally decomposed to CuO. Literature data [11] confirmed the one-step dehydration of four hydrated copper gentisate complex. The tetrahydrate of gentisate of Cd(II) heated in air is stable up to 30 °C. Above this temperature, cadmium compound is dehydrated in two steps losing 2.5 and 1.5 water molecules, respectively (Fig. 2b). The observed mass loss for total dehydration process is equal 14.48% (calc. 14.68%). The loss of all water molecules leads to creation of anhydrous compound, which gradually decomposes to CdO with formation intermediate, unstable compounds (180–415 °C). In the case of all investigated complexes, the dehydration process is endothermic, whereas the combustion of organic ligand is accompanied by strong exo-effects seen on the DSC curves. The observed various ways of thermal decomposition of analyzed 2,5-dihydroxybenzoates may be a result from the influence of central ions on properties of complexes.

DFT calculations

Atom assignment for two conformers of gentisic acid and its sodium, copper and cadmium salts with the values of their energy and dipole moments are shown in Table 3. The calculations were performed with use of B3LYP/6-311++G(d,p) method (for Cu and Cd complexes mixed basis set was used – 6-31++G(d,p)+LANL2DZ). Fourteen conformers of gentisic acid were taken into account during the calculations. No imaginary frequencies were found. The appropriate structures with the relative energies (in kcal/mol) are shown in Fig. 3. The conformers that do not have ability to create the intramolecular hydrogen bonds between the carboxylic and hydroxyl groups have the highest energy (nos. IX–XIV). The next two conformers, VII and VIII, form the intramolecular bonds which involve the hydrogen atom from the —OH carboxylic group and oxygen atom from the —OH substituent in the ortho position (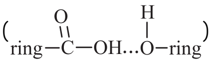 $\text{ring}-\overset{\overset{O}{\|}}{C}-OH\ldots\overset{\overset{H}{|}}{O}-\text{ring}$). The conformers nos. V and VI possess the intramolecular hydrogen bonds between the carbonyl group and the hydroxyl substituent (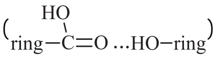 $\text{ring}-\overset{\overset{HO}{\backslash}}{C}{=}O\ldots HO-\text{ring}$) which causes the formation of so called quasi-aromatic ring. In the structures of gentisic acid molecules nos. III and IV the intramolecular hydrogen bonds exist between the oxygen of the —OH carboxylic part and the hydrogen atom of the hydroxyl substituent (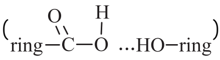 $\text{ring}-\overset{\overset{O}{\backslash\backslash}}{C}-\overset{\overset{H}{|}}{O}\ldots HO-\text{ring}$). For the structures with the lowest energy (I and II) the hydrogen bond is identical as hydrogen bond in structures V and VI. Depending on the hydrogen atom orientation in the carboxylic group one can observe the difference between aforementioned pairs of conformers. In the structures V and VI

Table 1
The values of weight percentages of carbon, hydrogen and metal in copper and cadmium gentisates.

Formula	Content C[a] (%)			Content H[a] (%)			Content M[b] (%)	
	Experimental	Theoretical	Lit. [10]	Experimental	Theoretical	Lit. [10]	Experimental	Theoretical
Copper(II) gentisate $(C_7H_5O_4)_2Cu\cdot4H_2O$	37.77–37.90	37.68	37.49	4.17–4.16	4.15	4.05	14.97	14.38
Cadmium(II) gentisate $(C_7H_5O_4)_2Cd\cdot4H_2O$	33.93–33.77	33.96	34.79	3.74–3.69	3.74	3.49	23.56	22.92

[a] Carbon (C) and hydrogen (H) determined from elemental analysis.

[b] Metal (M) content determined from TG curves.

Table 2
Thermal data of decomposition of Cu(II) and Cd(II) complexes with gentisic acid (air atmosphere).

Complex	ΔT_1 (°C)	Mass loss (%)			n	T_2 (°C)	Residue (%)		Final product of decomposition
		Calc.	Found	Lit. [10]			Calc.	Found	
$CuL_2{\cdot}4H_2O$	30–150	16.31	16.22	16.0	4	150–410	18.01	18.75	CuO
$CdL_2{\cdot}4H_2O$	30–140	9.71	9.96	14.5	2.5				
	140–180	4.97	4.52		1.5	180–415	26.18	26.92	CdO

L = $(C_7H_5O_4)^-$.
n – Number of water molecules being lost in dehydration endothermic step.
ΔT_1 – Temperature range of dehydration process.
T_2 – Temperature range of anhydrous complex decomposition.

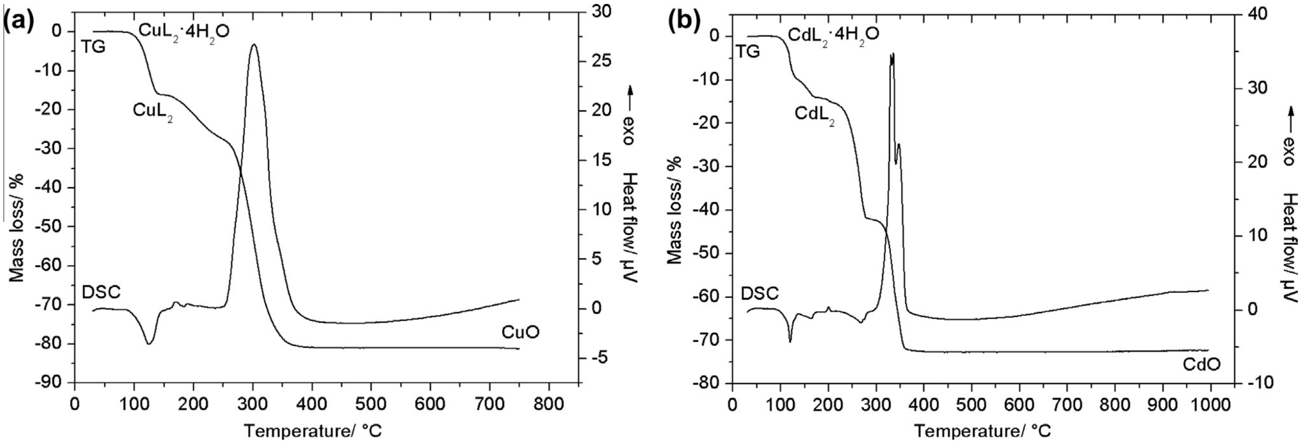

Fig. 2. TG and DSC curves of (a) copper gentisate $[Cu(C_7H_5O_4)_2]{\cdot}4H_2O$ and (b) cadmium gentisate $[Cd(C_7H_5O_4)_2]{\cdot}4H_2O$.

the hydrogen atom is directed toward the aromatic ring, whereas in the conformers I and II the hydrogen is directed to the outside of the molecule.

The difference between structure I and II consists in the spatial arrangement of hydroxyl substituent located near the aromatic carbon atom C5. The obtained results clearly show that the intramolecular hydrogen bonds affect the stability and π-electron delocalization. The strength of the intramolecular hydrogen bonds increases with the growth of the electron-donating and electron-withdrawing capacity of H-bond donor and H-bond acceptor, respectively. Consequently it leads to an increase of the π-electron delocalization in the quasi-ring.

The calculated structural parameters for studied molecules are gathered in Table 4. To compare the obtained results with the experimental data the Cambridge Structural Database was searched for the crystal structures of gentisic acid and gentisates. Several structures of gentisic acid were found [16–18] but only the most recent data were taken into account [18]. The quite good linear correlation between calculated and experimental [18] structural parameters were obtained. The correlation coefficients R for the distances between atoms in acid molecule are 0.994 and 0.949, respectively for structures I and II (appropriate values for angles between the bonds are 0.962 and 0.909). The above data indicate that the geometrical parameters of structure I (the one with the lowest energy) are in a better agreement with the experimentally obtained results. The main differences between theoretical and experimental bond lengths concern: the C4—H4 distance (the difference between theoretical and experimental values are Δ = 0.118 Å for the structure I and Δ = 0.120 Å for the structure II); the C6—H6 and O4—H5 (Δ = 0.100–0.104 Å), the C3—H3 (Δ = 0.073 Å), the O3—H2 (Δ = 0.073 Å), the C2—O3 (Δ = 0.019 Å) and the C5—O4 distances (Δ = 0.014–0.015 Å). The differences between experimental and theoretical bond lengths in the aromatic ring of gentisic acid are about ±0.013 Å. The carboxylic group is involved in the inter- and intramolecular hydrogen bonds formation. Although the intramolecular interactions were included during the calculations, the intermolecular effects were omitted. The C7—O2 bond length is lower in the calculated geometry in comparison with the experimental one by 0.013 Å for both I and II structures, while C7—O1 and O1—H1 calculated bond lengths are greater than experimental ones by about 0.032 and 0.058 Å, respectively. The distance between the O2 and H2 atoms is ~1.7 Å what suggests quite strong intramolecular hydrogen bonding and therefore stabilization of the structure of gentisic acid. The differences between the theoretical and experimental angles in the aromatic ring obtained for the structures of 2,5-dihydroxybenzoic acid are in the range from −0.92° to +0.96°. Greater changes are observed for C1—C7—O1 and C1—C7—O2 angles. The first one decreases by 1.19° and 1.16° in structure I and II, respectively, while the second one increases by 3.28° and 3.13°, respectively. Slightly changes are also observed for O1—C7—O2 angle: −2.09° (structure I) and −1.96° (structure II).

Two conformers in case of each metal gentisate molecules were calculated. The type of hydration and metal bonding for cadmium(II) and copper(II) gentisates were assumed on the basis of the results of elemental and thermogravimetric analyses as well as the literature data for crystal structure of zinc(II) gentisate [10]. Comparing the gentisic acid structure with the geometry of its sodium, copper and cadmium complexes the most visible changes in the distances between atoms as well as in the angles between bonds are observed in the region of carboxylic group. The increase of the oxygen—Metal (O—M) bonds follows the rise in the ionic radius of metal cations. The high impact of the intramolecular hydrogen bonds on the O—M distances was observed. In the case of sodium gentisate the bidentate structure of the carboxylate anion is quite symmetrical (O1—M: 2.215 and 2.212 Å; O2—M: 2.201 and 2.213 Å). However, in the structure of copper(II) and cadmium(II) gentisates the COO^- group is monodentate with

Table 3
Atom assignments for two conformers of gentisic acid and sodium, copper and cadmium gentsates with the values of their energy and dipole moments calculated by B3LYP/6-311++G(d,p). Energy in kcal/mol related to conformation of the structure I of lowest energy.

	Structures
Gentisic acid	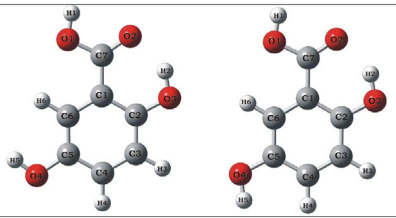
	E [kcal/mol] I 0.00000 II 0.46500
	Dipole moment [D] 2.801 2.114
Sodium gentisate	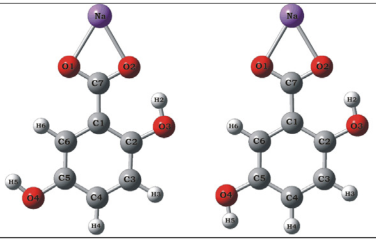
	E [kcal/mol] I 0.00000 II 0.71416
	Dipole moment [D] 8.979 6.570
Copper gentisate Structure I	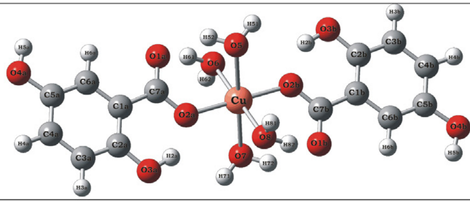
	E = 0.00000 kcal/mol
	Dipole moment = 0 D
Copper gentisate Structure II	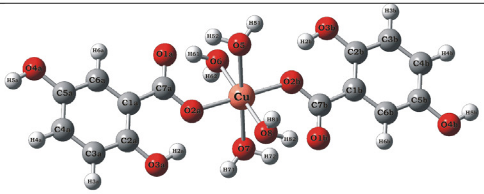
	E = 1.32304 kcal/mol
	Dipole moment = 0 D
Cadmium gentisate Structure I	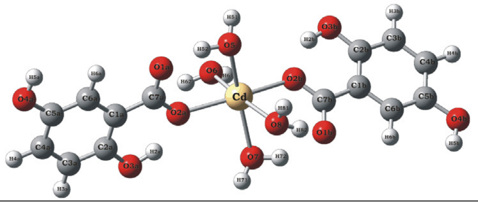
	E = 0.00000 kcal/mol
	Dipole moment = 1.208 D
Cadmium gentisate Structure II	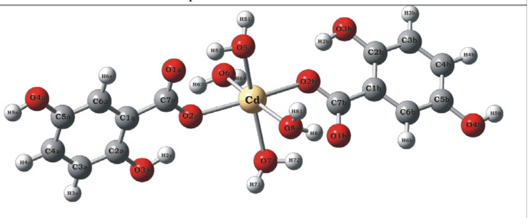
	E = 1.44899 kcal/mol
	Dipole moment = 2.286D

shorter O2—M bond and longer O1—M distance. Bigger differences between these bond lengths are observed in the case of copper gentisate than cadmium compound. Moreover, the oxygen O2 is engaged in the intramolecular hydrogen bond formation. The distance O2—H2 increases in the series of sodium → cadmium → copper gentisates → gentisic acid (i.e. 1.68 Å → 1.69–1.71 Å → 1.73 Å → 1.77 Å). These mean that there is a stronger intramolecular hydrogen bond in the molecules of metal gentisates than gentisic acid. Moreover, taking into account the three metal compounds the strongest intramolecular hydrogen bond exists in the sodium salt where the ionic type of metal bonding exists. The strength of the intramolecular hydrogen bond also reflects the calculated atomic charges gathered on the atoms involved in the quasi-aromatic ring formation. In the molecule of sodium gentisate the atomic charge on O2 atom is $-0.86e$ and on H2 atom was 0.22e, whereas for the structure of gentisic acid the following values are obtained: $-0.65e$ (O2) and 0.22e (H2). The type of metal coordination and the presence of the hydrogen bond affects the oxygen–carbon distances within the carboxylate group. The difference between the bond lengths of the carboxylate anion, i.e. C7—O2 and C7—O1 is lower in case of sodium gentisate ($\sim$0.03 Å) than copper gentisate ($\sim$0.05 Å). In case of cadmium gentisate some differences between the bond lengths and angles of the carboxylate group in the two coordinated ligands are observed. For example, the difference between the distance of C—O in the COO^- group is equal $\sim$0.06 Å in one of the gentisate ligand and $\sim$0.03 Å in the other ligand, or the values of angles between atoms C7—O2—M: $\sim$69° and $\sim$73° (the same situation occurs for I and II conformers of cadmium gentisate). Moreover, a significant increase in the C7—O1—H1/M angles is observed for gentisates of copper (by 17.18° – structure I and 17.23° – structure II) and cadmium (by 20.34° and 13.78° for structure I a and b ligands, respectively) in comparison with gentisic acid. However for sodium gentisate the decrease is noticed by 17.76° (structure I) and 17.71° (structure II). Taking into account the experimental structures of gentisic acid and zinc gentisate the C7—O1—H1/M angle increases by 22.03° in complex molecule. It confirms the tendency observed in theoretical data for transition metal complexes. Slightly smaller changes are noticed for O4—C5—C4 and O4—C5—C6 angles. The first one increases by 5.77° for copper, 5.71°/5.74° for cadmium (a/b molecules) and 0.37° for sodium salts if the structure I is taken into account. The second one decreases by 5.59°, 5.63°/5.60° and 0.37°, respectively. In experimental structure of zinc gentisate the same tendency is observed: O4—C5—C4 angle increases by 5.39° and O4—C5—C6 decreases by 5.03°, similarly to calculated structures of copper and cadmium gentisates. Other angles change only insignificantly.

The mutual arrangement of ligands in the copper and cadmium gentisate molecules is very surprising. Namely, in the structure of copper complex the two coordinated gentisate ligands are in one line and in the same plane, and the values of the geometrical parameters as well as atomic charges are identical in both ligands (therefore the dipole moment of the molecule is equal 0 D). On the other hand, in the cadmium complex the ligands are in substantially twisted planes to each other and they are not in lying one line. Moreover the bond lengths, angles and atomic charges differ slightly in the two gentisate ligands (the dipole moment of the structure I is 1.208 D and structure II is 2.286 D). The same type of metal coordination and the degree of hydration in cadmium and copper gentisates exist, but finally the kind of metal determines the spatial structure, geometrical parameters and atomic charge distribution of molecules.

The bond lengths in the aromatic ring of gentisic acid as well as its sodium, copper and cadmium salt molecules change very slightly. The values of the calculated aromatic indices [19] for each structures (Table 5) let us to draw the following conclusions: (1) the spatial arrangement of the substituents in the ring influences on the aromaticity of molecules (higher values of indices were obtained in case of structures II than I for gentisic acid and sodium

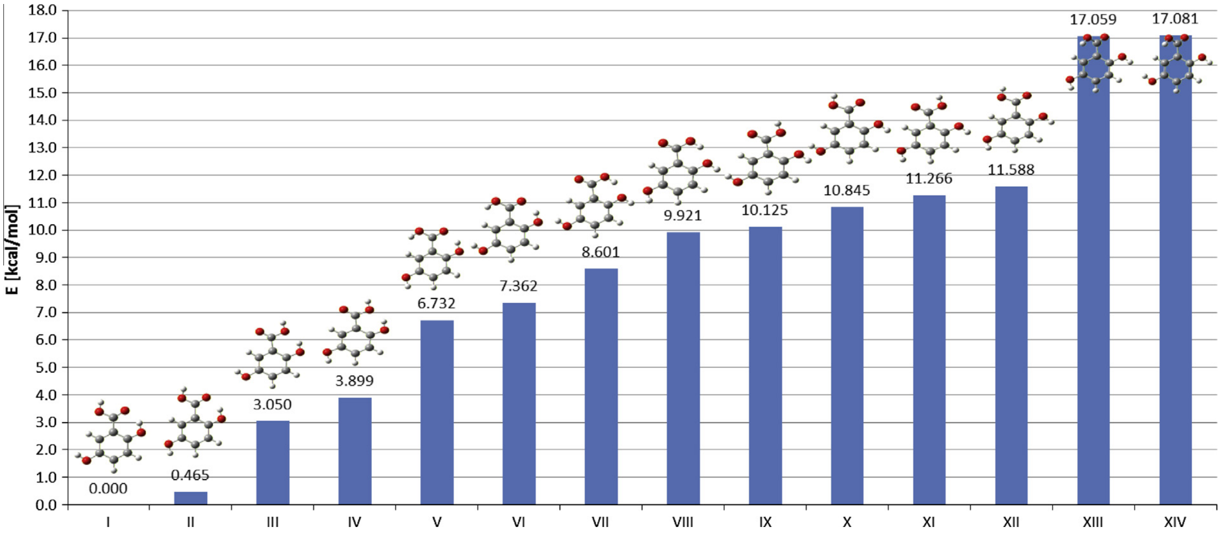

Fig. 3. The calculated [B3LYP/6-311++G(d,p)] energies of analyzed conformations of gentisic acid related to the conformation I (with the lowest energy).

gentisate, but for copper and cadmium gentisates the situation was opposite – structures I possessed higher automaticity indices than structures II), (2) the aromaticity of complexes varies depending on the kind of coordinated metal; (3) the gentisate molecules possess slightly higher aromaticity than gentisic acid. Comparing the values of indices obtained on the basis of experimental data for gentisic acid [18] and zinc gentisate [10] it is clearly seen that the aromaticity of metal complex molecule is higher that acid. It means that zinc cation causes increase in the delocalization of the electronic charge distribution in the aromatic ring of gentisate ligand and therefore higher stabilization of the π-electron system comparing with the gentisic acid structure. The structural parameters obtained by X-ray measurements of the respective compounds obtained in the form of crystals are the result of the existing intra- and intermolecular interactions, including hydrogen bonds. For the calculated structures the intramolecular interactions can be included but the intermolecular (especially long-distance) interactions are omitted. This is the reason why the aromaticity indices obtained for the calculated geometries should be carefully treated because they do not fully reflect the interactions in real structure. Moreover, it is interesting that in the case of the theoretically obtained structure of zinc gentisate with the lowest energy (structure I) the two hydroxyl substituents in the ring are directed toward the carboxylate group. Whereas in the experimental structure of zinc gentisate one of the hydroxyl substituent is directed toward COO^- anion, but the second one is situated in the opposite direction because of its involvement in the hydrogen bonding between the next gentisate ligand (Fig. 1). These intermolecular interactions are omitted during the calculations what probably affects the values of the aromaticity indices for theoretical structures. For the calculated structures the aromaticity increases in the order: gentisic acid < Cu < Na < Cd gentisates for structure I (in the case of BAC indices aromaticity of sodium gentisate is higher than acid and lower than copper salt molecule); for structure II all indices show increase of the aromaticity in the following series: acid < Cu < Cd < Na gentisates.

The changes in distances and angles are due of the replacement of H atom in carboxylic group by metal atom, which allows a better distribution of charges in the case of salt molecules. Atomic charges calculated by NBO method for gentisic acid and for sodium, copper and cadmium gentisate molecules are presented in Table 6. The formation of sodium gentisate causes significant changes on the charge distribution of atoms specially on the oxygen atoms of the COO function (NBO charges on O1/O2 atoms in structure I of gentisic acid equal −0.679/−0.651e and in sodium salt-structure I they are −0.799/−0.858e). Atomic charges on the carboxylic oxygen atoms decrease, so electronic density around those atoms increases. Partial atomic charges on C1 and C6 carbon atoms increase, while on other carbon atoms in the ring decrease in salt molecules in comparison with acid. The total charge of aromatic ring as well as carboxylate group are also calculated and presented in Table 6. The negative values of charge of both COO^- group and aromatic ring significantly increase in the following order: gentisic acid < copper < cadmium < sodium gentisates. As regards to O3 and O4 oxygen atoms in hydroxyl substituents higher changes are observed on O3 atom, though around both of them electronic density increases in comparison with acid structure. The positive charge on H2 and H5 atoms significantly increases in copper and cadmium gentisates in comparison with gentisic acid and its sodium salt. In sodium gentisate molecule lower atomic charges are observed on H2 and H5 atoms than on those atoms in acid molecule. The great positive charge is noticed on H4 atom in gentisic acid as well as in sodium gentisate, but in copper and cadmium complexes the decrease of this charge by about 0.25e is noticed. Some differences in atom charges are observed also in water molecules coordinated to copper and cadmium atoms. In cadmium gentisate there are four water molecules with different charges on atoms, each molecule has differ charge distribution. While in copper salt two molecules of water have the same charges on atoms and other two also have the same charge distribution, but differ from the first one. It is interesting to notice that in copper salt two molecules of gentisate ligand coordinated to Cu(II) atom have identical charges on atoms, bond lengths and angles between bonds. However cadmium gentisate contains two different molecules of gentisate ligand.

IR and Raman spectra

The FT-IR and FT-Raman spectra of gentisic acid and sodium, copper and cadmium gentisates were recorded and the wavenumbers, intensities and assignments of selected bands occurring in the experimental as well as calculated spectra are gathered in Table 7. Exemplary FT-IR and Raman spectra of cadmium gentisate is presented in Fig. 4. The bands are numbered along with the notation used by Varsányi [20]. A good correlation between experimental and theoretical wavenumbers in IR spectra of gentisic acid as well

Table 4
Calculated bond lengths and angles of gentisic acid and sodium, copper and cadmium gentisates.

Atoms	Gentisic acid			Sodium gentisate		Copper gentisate		Cadmium gentisate		Zinc gentisate
	Exp. [18]	Theoretical data		Theoretical data		Theoretical data		Theoretical data		
		Struct. I	Struct. II	Struct. I	Struct. II	Struct. I	Struct. II	Struct. I	Struct. II	Exp. [10]
Bond length (Å)										
C1—C2	1.402	1.412	1.415	1.410	1.414	1.414	1.411	1.413[a] 1.414[b]	1.410 1.411	1.409 1.409
C2—C3	1.403	1.402	1.399	1.403	1.399	1.399	1.402	1.398 1.399	1.401 1.402	1.388 1.388
C3—C4	1.376	1.381	1.385	1.385	1.388	1.387	1.383	1.388 1.387	1.384 1.383	1.386 1.386
C4—C5	1.398	1.404	1.402	1.400	1.399	1.400	1.402	1.399 1.400	1.400 1.401	1.394 1.394
C5—C6	1.383	1.381	1.383	1.384	1.385	1.384	1.382	1.385 1.385	1.383 1.383	1.380 1.380
C6—C1	1.407	1.411	1.406	1.405	1.401	1.404	1.408	1.402 1.403	1.407 1.408	1.392 1.392
C4—H4	0.966	1.084	1.086	1.084	1.087	1.086	1.084	1.087 1.087	1.084 1.084	0.968 0.968
C3—H3	1.010	1.083	1.083	1.083	1.083	1.083	1.083	1.083 1.083	1.083 1.083	0.971 0.971
C2—O3	1.366	1.347	1.347	1.351	1.351	1.353	1.352	1.356 1.353	1.355 1.353	1.369 1.369
C1—C7	1.474	1.464	1.467	1.489	1.492	1.486	1.483	1.493 1.487	1.490 1.485	1.493 1.493
C6—H6	0.980	1.084	1.081	1.085	1.082	1.082	1.085	1.082 1.082	1.085 1.085	0.856 0.856
C5—O4	1.387	1.372	1.373	1.379	1.379	1.375	1.374	1.376 1.376	1.376 1.375	1.384 1.384
O4—H5	0.862	0.963	0.962	0.962	0.962	0.962	0.963	0.962 0.962	0.963 0.963	0.726 0.726
O3—H2	0.908	0.980	0.980	0.989	0.989	0.980	0.980	0.984 0.983	0.984 0.983	0.846 0.846
C7—O2	1.238	1.225	1.225	1.291	1.291	1.301	1.300	1.302 1.293	1.301 1.293	1.295 1.295
C7—O1	1.316	1.351	1.348	1.261	1.259	1.251	1.252	1.245 1.258	1.247 1.260	1.259 1.259
O1—H1/M	0.911	0.969	0.969	2.215	2.212	3.135	3.137	3.430 3.253	3.434 3.261	3.370 3.370
O2—H1/M	–	–	–	2.210	2.213	1.972	1.971	2.243 2.274	2.241 2.273	2.051 2.051
O2—H2	1.753	1.774	1.771	1.679	1.672	1.728	1.724	1.703 1.686	1.707 1.692	1.742 1.742
Angle (°)										
C1—C2—C3	119.47	118.77	118.69	118.98	118.93	118.87	118.93	119.13 119.02	119.18 119.09	119.88 119.88
C2—C3—C4	120.13	120.78	120.63	120.85	120.64	120.74	120.92	120.64 120.65	120.83 120.82	120.65 120.65
C3—C4—C5	120.49	120.61	120.77	120.26	120.48	120.52	120.34	120.42 120.65	120.23 120.33	119.57 119.57
C4—C5—C6	120.38	119.57	119.45	119.57	119.48	119.39	119.49	119.47 119.43	119.57 119.53	120.02 120.02
C5—C6—C1	119.53	120.49	120.45	120.90	120.78	120.84	120.91	120.89 120.84	120.98 120.91	121.15 121.15
C6—C1—C2	119.99	119.79	120.02	119.44	119.69	119.64	119.41	119.45 119.55	119.22 119.32	118.65 118.65
H4—C4—C5	119.14	118.70	119.84	118.98	120.00	120.01	118.91	120.05 120.00	118.98 118.91	121.21 121.21
H4—C4—C3	120.32	120.69	119.39	120.76	119.51	119.47	120.75	119.53 119.48	120.79 120.76	118.98 118.98
H3—C3—C4	121.56	120.99	120.97	120.82	120.84	120.86	120.86	120.85 120.86	120.84 120.86	125.67 125.67
H3—C3—C2	118.31	118.24	118.40	118.33	118.52	118.40	118.22	118.52 118.49	118.34 118.32	112.95 112.95
C5—C6—H6	122.66	120.80	119.61	121.49	120.38	120.22	121.39	120.22 120.22	121.36 121.38	121.26 121.26
H6—C6—C1	117.81	118.72	119.94	117.62	118.84	118.94	117.71	118.90 118.94	117.66 117.71	117.39 117.39
C3—C2—O3	117.30	117.74	117.82	118.20	118.26	117.53	117.46	117.92 117.88	117.85 117.80	118.88 118.88
C1—C2—O3	123.23	123.49	123.49	122.83	122.81	123.61	123.61	122.95 123.10	122.97 123.11	121.26 121.26
O4—C5—C6	122.08	123.53	117.87	123.14	118.01	117.94	123.38	117.90 117.93	123.23 123.34	117.05 117.05

(*continued on next page*)

Table 4 (*continued*)

Atoms	Gentisic acid			Sodium gentisate		Copper gentisate		Cadmium gentisate		Zinc gentisate
	Exp. [18]	Theoretical data		Theoretical data		Theoretical data		Theoretical data		
		Struct. I	Struct. II	Struct. I	Struct. II	Struct. I	Struct. II	Struct. I	Struct. II	Exp. [10]
O4—C5—C4	117.54	116.91	122.68	117.28	122.52	122.68	117.13	122.62 122.65	117.21 117.13	122.93 122.93
C2—O3—H2	105.63	108.01	107.93	105.81	105.74	106.90	106.93	105.47 106.05	105.52 106.07	104.83 104.83
C2—C1—C7	119.38	118.93	118.82	121.32	121.10	122.22	122.40	122.05 121.76	122.26 121.93	121.23 121.23
C7—C1—C6	120.63	121.28	121.17	119.24	119.20	118.14	118.19	118.49 118.69	118.53 118.75	120.11 120.11
C1—C7—O1	115.93	114.74	114.77	120.33	120.38	116.29	116.37	116.45 117.33	116.52 117.41	116.40 116.40
C1—C7—O2	121.26	124.54	124.39	117.87	117.80	121.07	121.04	119.96 120.19	119.92 120.14	119.77 119.77
C7—O2—M	–	–	–	88.59	88.44	67.98	67.92	69.01 73.47	68.87 73.30	64.61 64.61
C7—O1—H1/M	108.02	106.86	106.96	89.10	89.25	124.04	124.19	127.20 120.64	127.42 120.97	130.05 130.05
O1—C7—O2	122.81	120.72	120.85	121.80	121.82	122.64	122.59	123.59 122.49	123.56 122.45	123.80 123.80
C5—O4—H5	108.19	109.92	109.94	109.20	109.41	109.76	109.62	109.66 109.73	109.47 109.57	104.72 104.72

[a] Two molecules of gentisate ligand coordinated to copper(II) or cadmium(II) atom, in copper(II) gentisate there are the same values of distances between atoms and angles between bonds in a molecules.

[b] Two molecules of gentisate ligand coordinated to copper(II) or cadmium(II) atom, in copper(II) gentisate there are the same values of distances between atoms and angles between bonds in b molecules.

Table 5
Aromaticity indices calculated on the basis of the theoretical as well as the experimental geometries of gentisic acid and sodium, copper, cadmium and zinc gentisates.

Indices	Gentisic acid			Sodium gentisate		Copper gentisate		Cadmium gentisate		Zinc gentisate
	Exp.[18]	Theoretical data		Theoretical data		Theoretical data		Theoretical data		
		Struct. I	Struct. II	Struct. I	Struct. II	Struct. I	Struct. II	Struct. I	Struct. II	Exp. [10]
HOMA	0.955	0.929	0.940	0.950	0.953	0.948 0.948	0.941 0.941	0.955 0.949	0.949 0.942	0.976
A_j	0.985	0.981	0.985	0.989	0.990	0.988 0.988	0.985 0.985	0.990 0.989	0.987 0.986	0.991
BAC	0.844	0.827	0.857	0.874	0.886	0.876 0.876	0.850 0.850	0.888 0.880	0.866 0.856	0.883
I_6	90.43	89.12	90.52	91.66	92.09	91.51 91.51	90.36 90.36	92.28 91.78	91.18 90.60	92.52

as its metal complexes were obtained. For example, the correlation coefficients are equal $R = 0.995$ and 0.996 for I and II structures of gentisic acid and $R = 0.995$ for both structures I and II of sodium gentisate molecules. Comparing FT-IR spectra of gentisic acid and its metal complexes one can observed that some bands characteristic for acid spectra disappeared in the spectra of gentisates, namely: $\upsilon(OH)_{COOH}$ stretching vibration band at 3130 cm^{-1} (IR) – appropriate band in calculated spectra is at 3767 cm^{-1} (for I and II structures), the band of $\beta(OH)_{COOH}$ in-plane deformation at 1204 cm^{-1} (in IR exp. spectrum) and at 1284; 1281 cm^{-1} (in IR spectrum calculated for I and II structures) and $\gamma(OH)_{COOH}$ at 854 cm^{-1} (IR exp.) and 572; 575 cm^{-1} (IR calc. I and II structures). The bands assigned to the symmetric stretching vibrations $\nu(C{=}O)$ at 1668 cm^{-1} (IR exp.), 1664 cm^{-1} (Raman) and 1730; 1731 cm^{-1} (IR calc.; I and II structures), $\beta(C{=}O)$ at 756 cm^{-1} (IR exp.), 751 cm^{-1} (Raman) and 738; 736 cm^{-1} (calc. I and II struct.) also decline. On the other hand the appearance of the bands connected with carboxylate ion is noticed in the spectra of gentisates. The band of $\beta_{as}(COO^-)$ in plane deformations occurs at 598 cm^{-1} (IR exp.) and at 576 cm^{-1} (IR calc. for both I and II structures) for Na gentisate. The increase of wavenumbers of this band is observed in the series Na < Cd < Cu gentisates. The band of $\beta_s(COO^-)$ in the IR spectra of sodium gentisate occurs at 887 cm^{-1} and it is shifted toward lower wavenumbers in copper salt spectra (880 cm^{-1}) as well as toward higher wavenumbers in the IR spectra of Cd gentisate (891 cm^{-1}). The wavenumbers of band assigned to the symmetric stretching vibrations of the carboxylate anion $\nu_s(COO^-)$ occurs in the IR spectra of sodium, copper and cadmium gentisates in the range of 1366–1385 cm^{-1}. The bands assigned to asymmetric stretching vibrations $\nu_{as}(COO^-)$ occur in the range 1587–1566 cm^{-1} (IR exp.), 1596–1563 (Raman) and the wavenumbers decrease in the series: Na > Cd > Cu gentisates. In calculated spectra this band changes from 1595 to 1560 cm^{-1} but it is difficult to describe the tendency of the changes, because two ligands in the cadmium molecule demonstrate two extreme vibration bands from above mentioned range. The wavenumebrs of the out-of-plane bending modes of COO^- are located in the range of 691–687 cm^{-1} (IR exp.), 693–690 cm^{-1} (Raman), 827–813 cm^{-1} (IR calc.). On the basis of the difference between IR wavenumbers of asymmetric and symmetric stretching vibrations of carboxylate anion [$\Delta\nu(COO)$] the type of coordination of the COO^- group by metal ions in studied gentisates may be analyzed. According to Zelenak et al. [21] the mode of carboxylate binding can be ionic, monodentate, bidentate chelating or bridging according the series: $\Delta\nu(\text{chelating}) < \Delta\nu(\text{bridging}) \leqslant \Delta\nu(\text{ionic}) < \Delta\nu(\text{monodentate})$. The $\Delta\nu(COO)$ for sodium, cadmium and copper gentisates are as

Table 6
Data of NBO atomic charge analysis for gentisic acid and sodium, copper and cadmium gentisates.

Atoms	Gentisic acid		Sodium gentisate		Copper gentisate				Cadmium gentisate			
	Structure I	Structure II	Structure I	Structure II	Structure I		Structure II		Structure I		Structure II	
C1	−0.235	−0.231	−0.218	−0.214	−0.215[a]	−0.215[b]	−0.219	−0.219	−0.216	−0.211	−0.220	−0.214
C2	0.361	0.357	0.342	0.340	0.343	0.343	0.346	0.346	0.341	0.335	0.344	0.337
C3	−0.232	−0.234	−0.238	−0.241	−0.237	−0.237	−0.235	−0.235	−0.238	−0.239	−0.236	−0.237
C4	−0.190	−0.224	−0.211	−0.243	−0.232	−0.232	−0.199	−0.199	−0.234	−0.238	−0.200	−0.205
C5	0.281	0.279	0.273	0.272	0.277	0.277	0.279	0.279	0.276	0.276	0.278	0.278
C6	−0.228	−0.192	−0.230	−0.195	−0.189	−0.189	−0.225	−0.225	−0.190	−0.191	−0.225	−0.226
C7	0.796	0.798	0.776	0.777	0.810	0.810	0.809	0.809	0.810	0.811	0.808	0.810
O1	−0.679	−0.673	−0.799	−0.792	−0.746	−0.746	−0.753	−0.753	−0.775	−0.708	−0.781	−0.715
O2	−0.651	−0.651	−0.858	−0.859	−0.770	−0.770	−0.769	−0.769	−0.851	−0.881	−0.851	−0.880
O3	−0.673	−0.675	−0.697	−0.698	−0.686	−0.686	−0.685	−0.685	−0.692	−0.699	−0.690	−0.697
O4	−0.677	−0.676	−0.686	−0.684	−0.678	−0.678	−0.680	−0.680	−0.679	−0.680	−0.681	−0.682
H2	0.223	0.223	0.215	0.214	0.504	0.504	0.504	0.504	0.502	0.500	0.501	0.499
H3	0.221	0.204	0.214	0.197	0.219	0.219	0.219	0.219	0.218	0.216	0.218	0.217
H4	0.468	0.467	0.46	0.462	0.201	0.201	0.219	0.219	0.201	0.199	0.218	0.217
H5	0.221	0.237	0.222	0.237	0.465	0.465	0.467	0.467	0.464	0.464	0.467	0.467
H6	0.221	0.237	0.222	0.237	0.239	0.239	0.224	0.224	0.238	0.239	0.223	0.224
H1/M	0.489	0.488	0.925	0.925	1.088		1.088		1.554		1.555	
O5					−0.914		−0.914		−1.007		−1.007	
H51					0.491		0.491		0.484		0.484	
H52					0.512		0.512		0.510		0.510	
O6					−0.920		−0.920		−0.941		−0.942	
H61					0.501		0.501		0.492		0.493	
H62					0.482		0.483		0.494		0.495	
O7					−0.914		−0.914		−0.973		−0.973	
H71					0.512		0.512		0.509		0.508	
H72					0.491		0.491		0.486		0.486	
O8					−0.920		−0.920		−0.973		−0.972	
H81					0.501		0.501		0.487		0.487	
H82					0.482		0.483		0.509		0.508	
Total atomic charges												
Ring	−0.243	−0.245	−0.282	−0.281	−0.253	−0.253	−0.253	−0.253	−0.261	−0.268	−0.259	−0.267
COO	−0.534	−0.526	−0.881	−0.874	−0.706	−0.706	−0.713	−0.713	−0.816	−0.778	−0.824	−0.785

follows: 202, 200 and 187 cm^{-1}, respectively. The obtained values are close to each other. Due to the above mentioned rules the obtained values of $\Delta\nu$(COO) may indicate bridging chelating mode of the carboxylate binding for both cadmium and copper gentisates, not as expected monodentate binding. The spectroscopic criterion must be carefully treated because it was established on the basis of the wavenumbers of $\nu_{as}(COO^-)$ and $\nu_s(COO^-)$ bands from IR spectra of metal acetates. To be sure of the type of coordination the crystal structures of the studied compounds should be only discussed. The large discrepancies between the results of a spectroscopic criterion and the type of metal coordination was demonstrated for differently hydrated structures of the same compound [22]. The values of $\Delta\nu$(COO) were also calculated basing on the theoretical spectra of studied salts. The appropriate data amount to 201(I) and 209(II) for Na2,5-DHB; 207(I) and 215(II) for Cu(2,5-DHB)$_2$(H$_2$O)$_4$ and 215(Ia), 204(Ib) and 221(IIa), 212(IIb) cm^{-1} for cadmium gentisate. The values confirmed the established during the calculation monodentate type coordination. On the other hand according to Micera et al. [12] the value of $\Delta\nu$(COO) for copper complex with 2,4-DHBA equals 195 cm^{-1} may indicate non bonding interactions involving the carboxylate groups distinguish from the Mn, Co, Ni and Zn 2,4-DHBs, which display carboxylate absorption typical for monodentate coordination ($\Delta\nu$ = 140 cm^{-1}). Authors suggested that in the case of Cu complex the phenolic groups may be responsible for long intermolecular axial contacts toward the metal ion [12].

The influence of alkali metals on the vibrational structure of gentisic acid expresses also in the shifts of some other bands in the spectra of gentisates comparing with the spectra of acid. Namely, bands nos. 8b, 8a, 14, 7a, 13, 18b, 16a and 6a are located at higher wavenumbers in the spectra of metal complexes than in the spectra of acid. Whereas, bands nos. 19a, 19b, ν(CC) ~1420 cm^{-1}, 17b, 11, 12 and 6b are shifted toward lower wavenumbers in the spectra of gentisates comparing with the spectra of gentisic acid. The stretching vibrations υ(CC) bands numbered as 8a, 8b, 19a and 19b occur in the region 1650–1424 cm^{-1} (IR exp.), 1651–1642 cm^{-1} (Raman) and 1680–1482 cm^{-1} (IR calc.). The first two bands shift to higher values of wavenumbers in the following series: gentisic acid < sodium < copper < cadmium gentisates. The differences between appropriate band in experimental IR spectra of acid and cadmium salt are from 9 to 26 cm^{-1} for 8a and 8b, respectively. In the case of 19b and 19a bands the order is: sodium gentisate < gentisic acid < copper < cadmium gentisates. The shifts equal from 4–15 cm^{-1} (19b) to 20–32 cm^{-1} (19a). For 8b the order of changes is following gentisic acid < sodium < copper < cadmium gentisates, while for 8a gentisic acid < copper < cadmium < sodium salts. The wavenumbers of the bands connected with 7a-υ(CH) vibrations are in the range 1252–1238 cm^{-1} and they increase in sodium, copper and cadmium gentisates by 10–14 cm^{-1} in comparison with the gentisic acid spectra, while that of 11-γ(CH) occurring in the range 839–814 cm^{-1} decrease by 15 cm^{-1} (for cadmium gentisate) – 25 cm^{-1} (for copper salt). The other bands of aromatic ring are placed at about similar wavenumbers both in the spectrum of acid and salts.

The bands assigned to υ(OH) stretching vibrations of the substituent in the ring, which occur at (1) 3310 cm^{-1} (IR), (2) 3073 cm^{-1} (IR) and 3073 cm^{-1} (Raman) in the experimental spectrum of acid, in the spectra of gentisates are shifted toward higher wavenumbers [3483–3194 cm^{-1} (IR), 3075 cm^{-1} (Raman)]. It suggest weakening of the intermolecular hydrogen bonding in the metal complex molecules comparing with acid. In the calculated spectra the first band changes only a bit in the range 1–3 cm^{-1} (structure I)

Table 7
Wavenumbers (cm^{-1}), intensities and assignments of selected bands occurring in the experimental and calculated B3LYP/(6-311++G**) FT-IR and Raman spectra of gentisic acid as well as sodium, copper and cadmium gentisates.

Gentisic acid				Sodium gentisate				Copper gentisate				Cadmium gentisate				Assignment[a] [20]	
IR exp.	IR calc. (intensity)		Raman	IR exp.	IR calc. (intensity)		Raman	IR	IR calc. (intensity)		Raman	IR exp.	IR calc. (intensity)		Raman		
	Struct. I	Struct. II			Struct. I	Struct. II			Struct. I	Struct. II			Struct. I	Struct. II			
3310 s	3838 (65.0)	3842 (73.1)		3426 s	3841 (53.7)	3844 (58.4)		3422 vs	3839 (122.5)	3843 (156.1)		3483 s	3839 (57.3); 3839 (61.0)	3843 (60.0); 3843 (82.6)			$\nu(OH)_{ar}$
3130 s	3767 (119.9)	3767 (120.0)															ν(OH)
3073 s	3499 (267.2)	3498 (285.4)	3073 m		3318 (479.5)	3305 (514.1)	3075 m		3490 (1190.5)	3486 (1261.0)	3067 s	3194 s	3431 (472.4); 3411 (740.1)	3424 (513.6); 3401 (771.7)			$\nu(OH)_{ar}$
	3202 (2.0)	3218 (2.2)	2985 w		3195 (7.0)	3191 (5.8)	2986 m		3199 (10.1)	3195 (7.8)			3198 (5.0); 3197 (5.0)	3194 (4.2); 3193 (4.3)		20b	ν(CH)
	3187 (1.1)	3199 (1.9)			3180 (5.1)	3144 (21.8)			3184 (5.7)	3150 (39.2)			3184 (3.1); 3183 (3.9)	3149 (18.18); 3148 (19.71)			ν(CH)
	3185 (7.1)	3152 (13.4)			3171 (10.1)	3208 (3.4)			3177 (24.7)	3212 (10.6)			3176 (10.3); 3175 (10.8)	3212 (4.2); 3212 (4.5)			ν(CH)
1668 vs	1730 (397.4)	1731 (385.7)	1664 s														ν(C=O)
1624 m	1663 (68.3)	1671 (48.9)		1632 s	1670 (7.3)	1677 (15.4)	1642 w		1670 (16.7)	1677 (35.6)	1642 m	1650 sh	1673 (5.6); 1671 (8.0)	1680 (12.2); 1678 (17.6)	1651 vw	8b	ν(CC)
1595 m	1630 (42.4)	1625 (44.2)	1609 m		1641 (29.7)	1633 (24.2)		1614 m	1634 (102.8)	1628 (160.3)	1611 w	1611 sh	1641 (21.8); 1639 (7.4)	1632 (2.9); 1629 (43.3)		8a	ν(CC)
				1587 vs	1577 (379.3)	1584 (347.5)	1596 m	1566 vs	1565 (857.5)	1571 (771.4)	1563 m	1572 s	1590 (637.0); 1560 (366.5)	1595 (611.7); 1566 (331.1)			$\nu_{as}(COO^-)$
1497 s	1526 (181.0)	1515 (278.8)	1473 m	1491 vs	1528 (268.8)	1517 (375.3)	1498 vw	1493 s	1524 (281.9)	1515 (665.2)	1492 vw	1487 vs	1527 (208.9); 1525 (212.7)	1516 (343.4); 1515 (154.5)		19b	ν(CC)
1472 m	1483 (49.2)	1495 (9.2)	1445 w	1462 s	1495 (336.7)	1506 (233.7)	1455 w	1460 vs	1500 (837.5)	1508 (296.5)	1459 vw	1462 sh	1503 (362.0); 1493 (486.2)	1514 (360.2); 1503 (330.1)		19a	ν(CC)
1439 vs				1425 m				1400 s			1409 s	1401 sh					ν(CC)
1377 m	1419 (219.4)	1421 (190.7)	1350 m		1422 (99.9)	1422 (29.0)			1409 (59.7)	1407 (12.0)			1420 (86.0); 1415 (61.9)	1420 (15.6); 1415 (19.2)			β(CH)+β(OH)
				1385 s	1376 (304.1)	1375 (449.5)	1390 w	1366 vs	1358 (1094.2)	1356 (1666.9)	1363 m	1385 vs	1375 (383.5); 1356 (624.8)	1374 (501.9); 1354 (862.9)	1390 vw		$\nu_s(COO^-)$
1314 w	1399 (48.0)	1391 (34.6)	1307 s	1327 m	1348 (76.3)	1343 (53.8)		1326 sh	1353 (258.2)	1348 (22.2)	1330 w	1329 s	1352 (84.6); 1351 (73.7)	1346 (83.1); 1345 (23.5)	1325 vw	14	ν(CC)
1277 m	1298 (6.4)	1296 (8.4)	1291 sh	1286 sh	1298 (12.8)	1289 (63.5)	1291 s	1275 m	1299 (16.8)	1290 (222.3)	1287 s	1275 m	1299 (12.3); 1298 (6.5)	1290 (69.1); 1289 (122.6)			νC—(OH), $\nu C{-}(OH)_{ar}$
1240 s			1246 w	1248 s	1269 (151.3)	1273 (124.5)	1246 m	1250 s	1260 (332.3)	1264 (262.0)	1249 w	1236 s	1265 (164.3); 1260 (145.9)	1269 (124.8); 1265 (112.3)	1254 vw	7a	ν(CH)
	1284 (156.6)	1281 (213.1)															β(OH)
1190 vs	1236 (14.8)	1228 (19.8)	1199 vs	1191 sh	1228 (3.8)	1222 (2.7)	1194 w		1228 (0.3)	1222 (9.2)		1196 m	1230 (3.5); 1230 (1.1)	1223 (1.2); 1222 (2.7)		13	ν(CH)
1136 sh	1192 (345.0)	1202 (101.9)	1131 w	1130 w	1183 (186.1)	1192 (101.8)	1137 w	1138 m	1182 (516.6)	1193 (190.7)	1141 m	1132 m	1184 (43.7); 1183 (414.1)	1193 (96.9) 1192 (98.8)	1133 vw	18a	β(CH), $\beta(OH)_{ar}$
1074 m	1146 (18.6)	1153 (0.4)	1080 w	1078 w	1146 (41.1)	1149 (19.8)	1083 w	1084 s	1150 (119.1)	1153 (38.5)	1087 w	1084 w	1149 (43.3); 1148 (58.1)	1152 (20.9) 1151 (20.8)	1090 vw	18b	β(CH)
	1079 (65.9)	1081 (54.1)			1097 (4.2)	1097 (13.7)			1103 (29.5)	1103 (57.8)			1101 (2.6); 1101 (18.2)	1101 (11.9; 32.1)			
951 w	971 (0.2)	951 (26.7)	957 w	951 sh	959 (0.2)	936 (4.1)	942 m	945 m	968 (0.7)	945 (7.2)	948 w	943 m	967 (0.2); 964 (0.2)	943 (3.0) 940 (3.9)	944 vw	17b	γ(CH)
934 m	949 (7.1)	946 (1.4)	939 s	937 m	951 (12.7)	952 (31.9)			960 (91.0)	960 (143.7)			955 (20.1); 950 (29.0)	955 (44.4) 950 (53.5)		7b	γ(CH)
				887 w	835 (13.8)	835 (19.7)		880 w	821 (55.7)	820 (57.9)	886 vw	891 w	819 (28.9)	819 (24.2) 818 (34.9)			$\beta_s(COO^-)$

876 sh	865 (18.9)	892 (10.6)	878 w		890 (12.0)	906 (7.8)			887 (28.9)	905 (78.1)			890 (12.4); 889 (12.9)	908 (7.1) 908 (8.5)		5	γ(CH)
854 m																	γ(OH)
839 m	847 (21.1)	829 (33.8)	834 w	822 s	846 (17.3)	847 (87.6)	817 vs	816 m	847 (60.6)	832 (95.0)	821 m	822 s	848 (46.8); 844 (39.7)	830 (44.6) 826 (50.1)	826 vw	11	γ(CH)
797 s	809 (34.3)	806 (55.3)	802 s	787 s	795 (74.4)	793 (93.3)	798 w	785 s	790 (287.4)	789 (311.9)		785 s		800 (88.0)		12	α(CCC)
	784 (40.9)	789 (27.8)							761 (152.7)	762 (165.4)			786 (47.4) 772 (91.1)	788 (44.8) 773 (81.3)			γ(OH), γ(CH)
756 m	738 (21.7)	736 (20.3)	751 vs														β(C=O)
	717 (99.9)	715 (107.0)															γ(OH)ar
721 m			701 vw		702 (14.3)	700 (12.7)			707 (57.4)	704 (63.9)	732 w		702 (8.7)	699 (7.7) 698 (18.3)		1	α(CCC)
				687 m	808 (3.1)	827 (35.1)	690 m	687 m	812 (124.1)	813 (120.1)	693 w	691 m	821 (42.9) 813 (59.7)	818 (34.9) 815 (34.8)	693 vw		γ_{s}(COO^{-})
679 s			678 w														γ(C=O)
				598 vw	576 (10.8)	576 (0.4)		627 w	583 (67.6)	580 (0.1)	614 vw	619 vw	586 (33.5) 576 (13.3)	586 (15.1) 576 (3.4)	623 vw		β_{as}(COO^{-})
559 sh	691 (0.1)	692 (0.5)	558 w	573 vw	697 (0.4)	694 (1.5)	574 m	579 vw	699 (6.2)	697 (6.1)			698 (65.4) 697 (0.3)	696 (27.8; 48.0)		16a	α(CCC)
550 m	673 (48.3)	673 (49.0)		554 m	576 (10.8)	576 (0.4)		552 m				556 m				6a	φ(CC)
	572 (102.8)	575 (113.8)															γ(OH)
482 sh	539 (2.1)	538 (0.5)	486 s	492 w	559 (18.0)	556 (21.0)	492 s	478 w	559 (46.1)	557 (53.1)	481 m	494 m	562 (35.1) 559 (14.0)	559 (42.9) 556 (16.4)	498 vw	16b	φ(CC)
469 s	478 (0.2)	480 (0.4)	457 s	461 w	485 (2.7)	486 (8.0)	466 w	459 w	482 (5.6)	483 (15.5)		463 w	484 (1.3); 481 (0.2)	485 (3.9); 482 (1.2)		6b	α(CCC)
436 w	423 (23.9)	429 (4.6)	442 vw	432 w	442 (2.9)	446 (0.7)	443 w		442 (59.9)	444 (77.8)	431 vw		443 (8.7); 443 (7.1)	446 (8.2); 445 (2.1)			φ(CC)
405 w	398 (15.5)	395 (2.3)	406 w		426 (16.5)	424 (22.2)			419 (51.6)	416 (22.0)			435 (26.1); 421 (17.9)	432 (39.0); 418 (24.4)		9b	β(CH)

---

[a] ν – stretching vibrations, β – in-plane bending modes, γ – out-of-plane, φ – the aromatic ring out-of-plane bending modes, α – the aromatic ring in-plane bending modes.

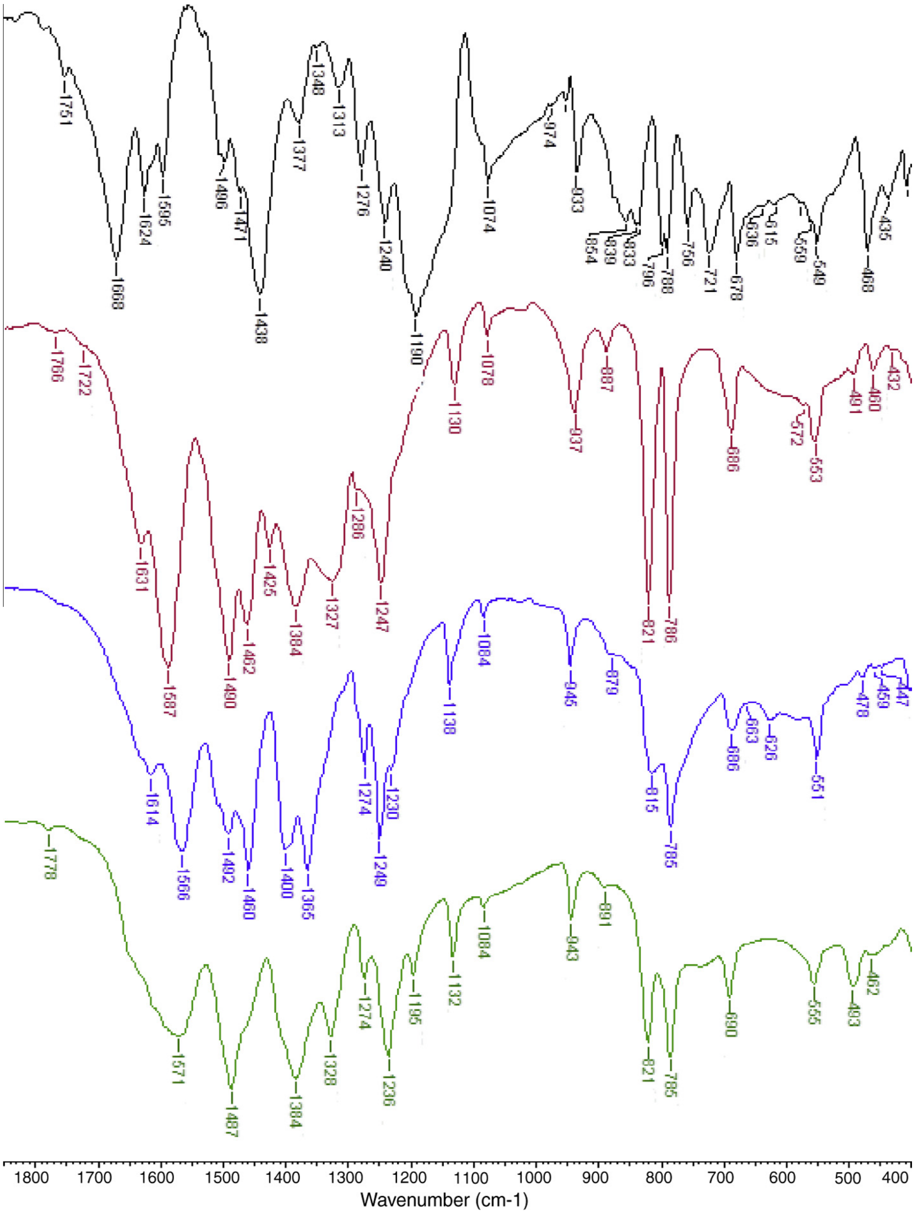

Fig. 4. FT-IR spectra of: (a) gentisic acid, (b) sodium gentisate, (c) copper(II) gentistate, and (d) cadmium(II) gentisate in the range of 1850–400 cm^{-1}.

and 1–2 cm^{-1} (structure II). However the other band appearing at 3499 cm^{-1} in structure I of acid is shifted toward lower wavenumbers by 181, 68/88 and 8 cm^{-1} respectively for sodium, cadmium (a/b ligands) and copper gentisates.

Conclusions

The elemental and thermal analyses revealed the formulas of synthesized complexes of gentisic acid with copper(II) and cadmium(II), ([Cu(C$_7$H$_5$O$_4$)$_2$]·4H$_2$O and [Cd(C$_7$H$_5$O$_4$)$_2$]·4H$_2$O), respectively. The successful calculations (in B3LYP/6-311++G** level) for gentisic acid and sodium, cadmium and copper gentisates were done. The monodentate type of coordination in copper and cadmium gentisates was established. Different conformations of molecules were studied in order to obtain the most stable ones. The orientation of the hydroxyl substituent in the aromatic ring strongly influence the inter- and intramolecular hydrogen bonds formation and therefore stabilization of the molecule. The high impact of the intramolecular hydrogen bonds on the O—Metal distances was observed. The calculations show that in the molecules of metal gentisates stronger intramolecular hydrogen bond existed than in gentisic acid. Moreover, taking into account the three metal compounds the strongest intramolecular hydrogen bond exists in the sodium salt where the ionic type of metal bonding exists. The mutual arrangement of ligands in the copper and cadmium gentisate molecules is surprising, because in the structure of copper complex the two coordinated gentisate ligands are in one line and in the same plane, and the values of the geometrical parameters as well as atomic charges are identical in both ligands. But, in the cadmium complex the ligands are in substantially twisted planes to each other and they are not in lying one line. Moreover the bond lengths, angles and atomic charges differ slightly in the two gentisate ligands.

The aromatic indices for studied compounds were calculated, but there is some factors that influence the values of these indices, inter alia: (1) the spatial arrangement of the substituents in the aromatic and the presence of the inter- and intramolecular hydrogen bonding, (2) the kind of coordinated metal, the type of metal coordination and the degree of hydration.

The detailed assignment of bands from the FT-IR and Raman spectra of gentisic acid and metal gentisates were done and the influence of metal cation on free ligand molecule was discussed.

Acknowledgements

Scientific work was financed from the budget for science in 2010–2013 years as a research project of Ministry of Science and Higher Education No. N N312 427 639.

Calculations by means of the Gaussian 09 set of codes were carried out in Wrocław Centre for Networking and Supercomputing (http://www.wcss.wroc.pl). Access to HPC machines and licensed software is gratefully acknowledged.

References

[1] S. Khadem, R.J. Marles, Molecules 15 (2010) 7985–8005.
[2] L. Vraslović, M. Kliškić, S. Gudić, I. Smoljko, Ind. J. Chem. Technol. 17 (2010) 89–94.
[3] M.A. Harish Nayaka, U.V. Sathisha, S.M. Dharmesh, Food Chem. 119 (2010) 1307–1312.
[4] J.F. Cunha, F.D. Campestrini, J.B. Calixto, A. Scremin, N. Paulino, Braz. J. Med. Biol. Res. 34 (2001) 381–388.
[5] S. Sharma, N. Khan, S. Sultana, Eur. J. Cancer Prev. 13 (2004) 53–63.
[6] K. Ashidate, M. Kawamura, D. Mimura, H. Tohda, S. Miyazaki, T. Teramoto, Y. Yamamoto, Y. Hirata, Eur. J. Pharmacol. 513 (2005) 173–179.
[7] I.S. Fernandez, P. Cuevas, J. Angulo, P. Lopez-Navajas, A. Canales-Mayordomo, R. Gonzales-Corrochano, R.M. Lozano, S. Valverde, J. Jimenez-Barbero, A. Romero, G. Gimenez-Gallego, J. Biol. Chem. 285 (2010) 11714–11729.
[8] R. Merkl, I. Hrádková, V. Filip, J. Šmidrkal, Czech J. Food Sci. 28 (4) (2010) 275–279.
[9] G. Levy, T. Tsuchiya, New England J. Med. 287 (9) (1972) 430–432.
[10] G. Micera, L.S. Erre, P. Piu, F. Cariati, G. Ciani, A. Sironi, Inorg. Chim. Acta 107 (1985) 223–227.
[11] J. Sokolik, B. Lučanská, G. Plesch, I. Tumová, A. Valent, P. Švec, J. Krätsmár-Šmogrovič, Collect. Czech. Chem. Commun. 58 (1993) 1363–1370.
[12] G. Micera, L.S. Erre, G. Ciani, A. Sironi, Inorg. Chim. Acta 108 (1985) L1–L2.
[13] A. Karaliota, V. Aletras, D. Hatzipanayioti, M. Kamariotaki, M. Potamianou, J. Mass Spectrom. 37 (2002) 760–763.
[14] C. Litos, A. Terzis, C. Raptopoulou, A. Rontoyianni, A. Karaliota, Polyhedron 25 (2006) 1337–1347.
[15] M.J. Frisch, G.W. Trucks, H.B. Schlegel, G.E. Scuseria, M.A. Robb, J.R. Cheeseman, G. Scalmani, V. Barone, B. Mennucci, G.A. Petersson, H. Nakatsuji, M. Caricato, X. Li, H.P. Hratchian, A.F. Izmaylov, J. Bloino, G. Zheng, J.L. Sonnenberg, M. Hada, M. Ehara, K. Toyota, R. Fukuda, J. Hasegawa, M. Ishida, T. Nakajima, Y. Honda, O. Kitao, H. Nakai, T. Vreven, J.A. Montgomery, Jr., J.E. Peralta, F. Ogliaro, M. Bearpark, J.J. Heyd, E. Brothers, K.N. Kudin, V.N. Staroverov, R. Kobayashi, J. Normand, K. Raghavachari, A. Rendell, J.C. Burant, S.S. Iyengar, J. Tomasi, M. Cossi, N. Rega, J.M. Millam, M. Klene, J.E. Knox, J.B. Cross, V. Bakken, C. Adamo, J. Jaramillo, R. Gomperts, R.E. Stratmann, O. Yazyev, A.J. Austin, R. Cammi, C. Pomelli, J.W. Ochterski, R.L. Martin, K. Morokuma, V.G. Zakrzewski, G.A. Voth, P. Salvador, J.J. Dannenberg, S. Dapprich, A.D. Daniels, Ö. Farkas, J.B. Foresman, J.V. Ortiz, J. Cioslowski, D.J. Fox, Gaussian 09, Revision D.01, Gaussian Inc., Wallingford, CT, 2009.
[16] M. Haisa, S. Kashino, S.-I. Hanada, K. Tanaka, S. Okazaki, M. Shibagaki, Acta Crystallogr., Sect. B: Struct. Crystallogr. Cryst. Chem. 38 (1982) 1480–1485.
[17] D.E. Cohen, J.B. Benedict, B. Morlan, D.T. Chiu, B. Kahr, Cryst. Growth Des. 7 (2007) 492–495.
[18] M.S. Adam, M.J. Gutmann, C.K. Leech, D.S. Middlemiss, A. Parkin, L.H. Thomas, C.C. Wilson, New J. Chem. 34 (2010) 85–91.
[19] M. Kalinowska, E. Siemieniuk, A. Kostro, W. Lewandowski, J. Mol. Struct. THEOCHEM 761 (2006) 129–141.
[20] G. Varsányi, Assignments for Vibrational Spectra of 700 Benzene Derivatives, Akademiai Kiado, Budapest, Hungary, 1973.
[21] V. Zelenak, Z. Vargova, K. Gyoryova, Spectrochim. Acta Part A 66 (2007) 262–272.
[22] T. Ishioka, Y. Shibata, M. Takahashi, I. Kanesaka, Y. Kitagawa, K.T. Nakamura, Spectrochim. Acta A 54 (1998) 1827–1835.